

Intruding the sealed land: Unique forbidden beta decays at zero momentum transfer

Chien-Yeah Seng^{1,2}, Ayala Glick-Magid^{2,3}, and Vincenzo Cirigliano³

¹*Facility for Rare Isotope Beams, Michigan State University, East Lansing, MI 48824, USA*

²*Department of Physics, University of Washington, Seattle, WA 98195-1560, USA and*

³*Institute for Nuclear Theory, University of Washington, Seattle, WA 98195-1550, USA*

(Dated: September 27, 2024)

We report the first study of the $\mathcal{O}(\alpha)$ structure-dependent electromagnetic radiative corrections to unique first-forbidden nuclear beta decays. We show that the insertion of angular momentum into the nuclear matrix element by the virtual/real photon exchange opens up the decay at vanishing nuclear recoil momentum which was forbidden at tree level, leading to a dramatic change in the decay spectrum not anticipated in existing studies. We discuss its implications for precision tests on the Standard Model and searches for new physics.

The standard classification of nuclear beta decays follows angular momentum and parity selection rules. Consider the tree-level amplitude that depends on the nuclear matrix element:

$$\langle J_f^{P_f}(\vec{p}_f) | J_W^\mu(0) | J_i^{P_i}(\vec{p}_i) \rangle, \quad (1)$$

where J_W^μ is the charged weak current, and $J_{i(f)}$, $P_{i(f)}$, $\vec{p}_{i(f)}$ denote the spin, parity, and momentum of the initial (final) nucleus. Decays that satisfy the selection rules: $|J_i - J_f| = 0, 1$ and $P_i = P_f$ are known as “allowed” beta decays, while the rest are known as “forbidden” decays as their tree-level transition matrix elements are kinematically suppressed. In particular, for decays with $|J_i - J_f| \geq 2$, the amplitude above survives only when the nuclear recoil momentum \vec{q} is non-zero, due to rotational invariance.

Allowed beta decays provide stringent tests of the Standard Model (SM) and probe physics beyond the Standard Model (BSM) [1], e.g. through the precise measurement of the Cabibbo-Kobayashi-Maskawa (CKM) matrix elements [2, 3], and by constraining exotic interactions [4–13]. On the other hand, forbidden decays have recently received increased attention due to their complementary role in probing new physics [14], e.g. exotic (non $V-A$) charged-current couplings (see Refs. [4, 6] for a mapping between the traditional Lee-Yang [15] nucleon-level interaction and the modern Standard Model Effective Field theory framework). It has recently been highlighted that measurements of the unique forbidden beta decay spectrum provide simultaneous access to both the Fierz term and the electron-neutrino angular correlation [16, 17]; the former is linear in the coefficients of new physics but lacks sensitivity to right-handed neutrino interactions, while the latter is sensitive to both left- and right-handed neutrino interactions but is quadratic in the new physics coefficients. As an example, we consider the unique first forbidden decay ($|J_i - J_f| = 2$, $P_i = -P_f$), whose leading order matrix element is suppressed linearly by the nuclear momentum transfer $\mathbf{q} \equiv |\vec{q}| = |\vec{p}_i - \vec{p}_f|$. The tree-level differential decay rate takes the form

$$d\Gamma_{\text{tree}} \propto \mathbf{q}^2 \left\{ 1 + b \frac{m_e}{E_e} + a \left[2\vec{\beta} \cdot \hat{p}_\nu - \hat{p}_\nu \cdot \hat{q} \vec{\beta} \cdot \hat{q} \right] \right\}, \quad (2)$$

where \mathbf{q}^2 comes from the nuclear matrix element squared, m_e (E_e) is the mass (energy) of the emitted electron, and $\vec{\beta} \equiv \vec{p}_e/E_e$. The observables depending on the BSM tensor coefficients $C_T^{(n)}$ [15, 18, 19] are the Fierz term $b = \pm \Re[(C_T + C_T')/C_A]$, and the angular correlation $a = -(1/5)(1 - (|C_T|^2 + |C_T'|^2)/|C_A|^2)$. The last term multiplied by a in the tree-level rate does not exist in allowed decays. This term prevents the angular correlation from vanishing as in the allowed decays when integrating over the angles, making the unique forbidden spectrum sensitive to a , and as a result, also to right-handed tensor couplings.

This observation has motivated a number of new experiments to study unique first-forbidden decays. Measurements of $^{90}\text{Sr}(0^+) \rightarrow ^{90}\text{Y}(2^-)$ and $^{90}\text{Y}(2^-) \rightarrow ^{90}\text{Zr}(0^+)$ are currently being conducted at the Hebrew University of Jerusalem, and these will be followed with measurements of $^{16}\text{N}(2^-) \rightarrow ^{16}\text{O}(0^+)$, with an aim for 10^{-3} accuracy [20–22]. Additionally, studies on $^{90}\text{Y}(2^-) \rightarrow ^{90}\text{Zr}(0^+)$ and $^{144}\text{Pr}(0^-) \rightarrow ^{144}\text{Nd}(2^+)$ are underway at the Oak Ridge National Laboratory, aiming for 1-2% accuracy at the first stage [23, 24]. However, similar to their allowed counterparts, one requires all the SM predictions of the forbidden decays to reach the same accuracy in order to maximize the discovery potential of the experiments. Existing theory analyses of forbidden beta decays focus mainly on calculations of tree-level transition amplitudes, Coulomb effects, shape factor and recoil corrections [25–59]. Existing shell model calculations of tree-level matrix elements typically have uncertainties spanning an order of magnitude [29, 37, 49], which will be improved with future *ab initio* calculations, e.g. [60]. However, an important missing piece in the program is the study of the full one-loop radiative correction (RC) to the forbidden decay amplitude; the latter is known to play a central role in the interpretation of precision beta decays, e.g. the extraction of V_{ud} [61–69], the nucleon axial coupling constant [70–73], and the correction to the beta spectrum [74–76].

In this Letter, we report the first study of the $\mathcal{O}(\alpha)$

RC to forbidden decays which leads to an interesting new observation: The usual statement that forbidden decay amplitudes with $|J_i - J_f| \geq 2$ vanish in the non-recoil limit is falsified by the RC due to the introduction of an extra current operator into the nuclear matrix element that alleviates the inhibition from the angular momentum difference. As a consequence, at small enough \mathbf{q} the RC amplitude actually overtakes Eq.(2) as the main contributor to the forbidden decay rate. The same effect can also be achieved with new light degrees of freedom (DOFs) in the BSM sector that take the role of the photon in the RC. Explicitly, the differential decay rate now takes the form:

$$d\Gamma \propto f_0 \mathbf{q}^0 + f_1 \mathbf{q}^1 + f_2 \mathbf{q}^2, \quad (3)$$

where the first two terms probe the SM RC and light new physics, while the third term probes the SM tree-level effects and heavy new physics. Therefore, the precise study of the $\mathbf{q} \rightarrow 0$ behavior of forbidden decays provides a unique opportunity to simultaneously probe higher-order SM physics as well as BSM physics, without being contaminated by the large SM tree-level uncertainty. We investigate this novel idea in detail and discuss future prospects.

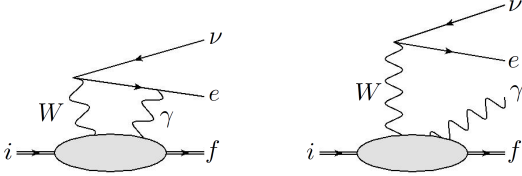


Figure 1: $\mathcal{O}(\alpha)$ Feynman diagrams that open up the forbidden nuclear transition at $\mathbf{q} = 0$.

We begin by studying the SM RC. It can be recognized that among all the $\mathcal{O}(\alpha)$ corrections, only the two diagrams in Fig.1, namely the γW -box diagram and the bremsstrahlung diagram with a photon emitted by the nucleus, can lead to a non-zero amplitude at $\mathbf{q} = 0$, since all other diagrams depend on the tree-level nuclear matrix element in Eq.(1) (although J_W^μ may be renormalized) which has to satisfy the same angular momentum and parity selection rules. Their corresponding amplitudes read (assuming β^- -decay) [64]:

$$\begin{aligned} \mathcal{M}_{\gamma W} &= \frac{G_F V_{ud}}{\sqrt{2}} e^2 L_\lambda \int \frac{d^4 k}{(2\pi)^4} \frac{M_W^2}{M_W^2 - k^2} \frac{1}{k^2 - m_\gamma^2 + i\epsilon} \\ &\times \frac{1}{(p_e - k)^2 - m_e^2 + i\epsilon} \{-2g^{\nu\lambda} p_e^\mu + g^{\mu\lambda} k^\nu + g^{\nu\lambda} k^\mu \\ &- g^{\mu\nu} k^\lambda - i\epsilon^{\mu\nu\alpha\lambda} k_\alpha\} T_{\mu\nu}(k) \\ \mathcal{M}_{\text{brem}} &= i \frac{G_F V_{ud}}{\sqrt{2}} e e^{\mu*} L^\nu T_{\mu\nu}(k), \end{aligned} \quad (4)$$

where $L_\lambda = \bar{u}_e \gamma_\lambda (1 - \gamma_5) v_\nu$ is the lepton current, and

$$T^{\mu\nu}(k) \equiv \int d^4 x e^{ik \cdot x} \langle \phi_f(-\vec{q}) | T [J_{\text{em}}^\mu(x) J_W^\nu(0)] | \phi_i(\vec{0}) \rangle \quad (5)$$

is a ‘‘generalized Compton tensor’’ involving the electromagnetic (em) and weak (W) currents, with external momenta $\vec{p}_i = \vec{0}$ and $\vec{p}_f = -\vec{q}$. We focus on the γW -box diagram that gives the dominant contribution as we show later.

To be concrete, let us concentrate on unique first-forbidden decays involving the transition $2^- \leftrightarrow 0^+$, in accordance with the planned experiments we mentioned in the introduction. The first important observation is that at $\mathbf{q} = 0$ the loop integral in $\mathcal{M}_{\gamma W}$ is dominated by small values of the virtual photon momentum k . This is seen by noticing that when k is large, one may take $p_e \rightarrow 0$ in the integrand which reduces the integral to:

$$\mathcal{M}_{\gamma W} \rightarrow \frac{G_F V_{ud}}{\sqrt{2}} e^2 L_\lambda \langle \phi_f(\vec{0}) | K^\lambda | \phi_i(\vec{0}) \rangle, \quad (6)$$

where

$$\begin{aligned} K^\lambda &\equiv \int \frac{d^4 k}{(2\pi)^4} \frac{M_W^2}{M_W^2 - k^2} \frac{1}{(k^2)^2} \{g^{\mu\lambda} k^\nu + g^{\nu\lambda} k^\mu \\ &- g^{\mu\nu} k^\lambda - i\epsilon^{\mu\nu\alpha\lambda} k_\alpha\} \int d^4 x e^{ik \cdot x} T \{J_\mu^{\text{em}}(x) J_\nu^W(0)\} \end{aligned} \quad (7)$$

No matter how complicated K^λ is, it remains an ordinary four-vector with no external momentum dependence, so $\langle \phi_f(\vec{0}) | K^\lambda | \phi_i(\vec{0}) \rangle$ must vanish due to rotational invariance given that $|J_i - J_f| = 2$. Hence, the integral is dominated by the small- k region, and more precisely the ultrasoft photon region in which $k^0 \sim |\mathbf{k}| \sim E_e$ (see Refs. [67, 68] for a discussion of radiative corrections to superallowed β decays in terms of various regions in photon virtuality). In the ultrasoft region, the main contribution to $T^{\mu\nu}(k)$ is from nuclear ground- and excited states $\{|X\rangle\}$, which allows us to rewrite it as:

$$\begin{aligned} T^{\mu\nu}(k) &\approx -i \sqrt{4M_i M_f} \sum_X \sum_{m_X} \\ &\left\{ \frac{\langle J_f m_f | J_{\text{em}}^\mu(\vec{k}) | J_X m_X \rangle \langle J_X m_X | J_W^\nu(-\vec{k}) | J_i m_i \rangle}{M_X - (M_f + k_0 + i\epsilon)} \right. \\ &\left. + \frac{\langle J_f m_f | J_W^\nu(-\vec{k}) | J_X m_X \rangle \langle J_X m_X | J_{\text{em}}^\mu(\vec{k}) | J_i m_i \rangle}{M_X - (M_i - k_0 + i\epsilon)} \right\} \end{aligned} \quad (8)$$

where we take $\vec{q} = 0$ and all states are normalized to 1.

In the small- k region, we can take $\mathbf{k}R$ as a small expansion parameter, where $\mathbf{k} \equiv |\vec{k}|$ and R is a typical nuclear radius. This allows us to apply the standard multipole expansion of the Fourier-transformed current operators

$J^\mu(\pm\vec{k})$ [77]:

$$\begin{aligned} J^0(\pm\vec{k}) &= \sqrt{4\pi} \sum_{J=0}^{\infty} (\mp i)^J [J] C_{J0}(\mathbf{k}) \\ \vec{J}(\pm\vec{k}) &= \pm\sqrt{4\pi} \sum_{J=0}^{\infty} (\mp i)^J [J] L_{J0}(\mathbf{k}) \vec{\epsilon}_0^* \\ &\quad -\sqrt{2\pi} \sum_{\lambda=\pm 1} \sum_{J=1}^{\infty} (\mp i)^J [J] (\lambda M_{J\lambda}(\mathbf{k}) \mp E_{J\lambda}(\mathbf{k})) \vec{\epsilon}_\lambda^*, \end{aligned} \quad (9)$$

where $[J] = \sqrt{2J+1}$; here we introduce C , L , M , E as the Coulomb, longitudinal, transverse magnetic and transverse electric multipole operators respectively, with the polarization vectors $\vec{\epsilon}_0 = \hat{z}$, $\vec{\epsilon}_{\pm 1} = \mp(\hat{x} \pm i\hat{y})/\sqrt{2}$ defined in a coordinate frame with $\hat{z} \equiv \hat{k}$. Following the power counting in the multipole formalism, we find that the leading contributors to $T^{\mu\nu}$ for the $i(2_g^-) \rightarrow f(0_g^+)$ transition (here g stands for ground state) involve the ground states $i(2_g^-)$, $f(0_g^+)$ and the $J=1$ excited states $i(1_X^+)$, $f(1_X^-)$. While the full leading expression of $T^{\mu\nu}$ can be found in the supplementary material, we observe that the ground state contribution involves the electromagnetic Coulomb operator and is enhanced by the atomic number Z . It gives rise to:

$$\begin{aligned} T^{0i}(m) &\approx i\sqrt{16\pi M_i M_f} \mathbf{k} \mathbf{C}_{\text{tree}} \left(\frac{Z_f \mathbf{C}_{\gamma g}^f}{k_0 + i\varepsilon} - \frac{Z_i \mathbf{C}_{\gamma g}^i}{k_0 - i\varepsilon} \right) \times \\ &\quad \left\{ S_{0m}(\theta) (\vec{\epsilon}_0^*)^i \mp \frac{\sqrt{3}}{2} (S_{\mp 1m}(\theta) (\vec{\epsilon}_1^*)^i + S_{\pm 1m}(\theta) (\vec{\epsilon}_{-1}^*)^i) \right\} \end{aligned} \quad (10)$$

where the upper (lower) sign corresponds to the $i(2^-) \rightarrow f(0^+)$ ($i(0^+) \rightarrow f(2^-)$) decay, $\{\mathbf{C}_{\text{tree}}, \mathbf{C}_{\gamma g}^{i,f}\}$ are reduced nuclear matrix elements (non-zero at $\mathbf{k}=0$) defined in Table SI in the supplementary material, and m is the magnetic quantum number of the external 2^- nuclear state along \hat{p}_e . The matrix $S(\theta)$ (where $\theta = \cos^{-1}(\hat{p}_e \cdot \hat{k})$), whose explicit expression can be found in the supplementary material, is responsible for the rotation of the 2^- spin state along \hat{p}_e to that along \hat{k} ; the latter is needed for the proper application of the Wigner-Eckart theorem involving the multipole operators.

We may now evaluate the box diagram amplitude $\mathcal{M}_{\gamma W}$. First, to suppress the dependence on physics at large k , we make use of our previous argument that the amplitude vanishes at $p_e \rightarrow 0$ to write the amplitude in the subtracted form

$$\mathcal{M}_{\gamma W}(p_e) = \mathcal{M}_{\gamma W}(p_e) - \mathcal{M}_{\gamma W}(0). \quad (11)$$

We then substitute the leading small- k expression of $T^{\mu\nu}$ given in Eq.(8) in the integrand appearing in both $\mathcal{M}_{\gamma W}(p_e)$ and $\mathcal{M}_{\gamma W}(0)$. We may then evaluate the k_0 -integral by closing up the contour from the lower half in the complex k_0 -plane (which is an arbitrary choice;

one may also choose the upper half). In doing so we observe that, only the residue at $k_0 = -i\varepsilon$ is enhanced by the atomic number Z_f at small \mathbf{k} ; picking up other poles always leads to a partial cancellation between the two elastic terms in Eq.(10), $Z_f/k_0 - Z_i/k_0 = 1/k_0$, that loses such an enhancement. It is also easy to see that the bremsstrahlung amplitude $\mathcal{M}_{\text{brem}}$ does not receive such an enhancement, because there the $\pm i\varepsilon$ in $T^{\mu\nu}$ does not play a role and the partial cancellation always takes place. Retaining only the Z_f -enhanced term [78] leads to, after straightforward algebra:

$$\mathcal{M}_{\gamma W} \approx -\frac{G_F V_{ud}}{\sqrt{2}} e^2 \left(L^0 I^0 - \vec{L} \cdot \hat{p}_e I' \right), \quad (12)$$

where we are left with two scalar integrals:

$$\begin{aligned} I^0 &= \frac{Z_f \sqrt{16\pi M_i M_f}}{2\pi^2} \mathbf{p}_e \int_0^\pi d\theta \sin\theta \cos\theta S_{0m}(\theta) \\ &\quad \times \int_0^\infty d\mathbf{k} \frac{\mathbf{C}_{\text{tree}}(\mathbf{k}) \mathbf{C}_{\gamma g}^f(\mathbf{k})}{\mathbf{k} - 2\mathbf{p}_e \cos\theta} \\ I' &= \frac{Z_f \sqrt{16\pi M_i M_f}}{4\pi^2} \int_0^\pi d\theta \sin\theta \int_0^\infty d\mathbf{k} \frac{\mathbf{C}_{\text{tree}}(\mathbf{k}) \mathbf{C}_{\gamma g}^f(\mathbf{k})}{\mathbf{k} - 2\mathbf{p}_e \cos\theta} \\ &\quad \times \left\{ 2E_e \cos\theta S_{0m}(\theta) \mp \sqrt{\frac{3}{2}} S_{\mp 1m}(\theta) \sin\theta (\mathbf{p}_e \cos\theta - E_e) \right. \\ &\quad \left. \mp \sqrt{\frac{3}{2}} S_{\pm 1m}(\theta) \sin\theta (\mathbf{p}_e \cos\theta + E_e) \right\}, \end{aligned} \quad (13)$$

where $\mathbf{p}_e \equiv |\vec{p}_e|$.

The above integrals are logarithmically divergent in the ultraviolet. In an effective field theory (EFT) approach, one would regulate the integrals in dimensional regularization and reabsorb the divergence through terms from the potential photon region [67]. Here, however, we are interested in a first rough estimate and therefore introduce the \mathbf{k} -dependence of $\mathbf{C}_{\gamma g}^f$ and \mathbf{C}_{tree} as a means to ensure the ultraviolet-finiteness of the \mathbf{k} -integral and obtain a model-dependent value for the corresponding EFT coupling. In principle, $\mathbf{C}_{\gamma g}^f$ can be inferred from the nuclear charge distribution data and the latter requires nuclear structure calculations, but in this Letter we resort to a simple approximation for illustration. First, we know the small- \mathbf{k} expansion of the charge form factor: $\mathbf{C}_{\gamma g}(\mathbf{k}) = 1 - \mathbf{k}^2 R_C^2/6 + \dots$, where R_C is the nuclear root-mean-square charge radius. So, we adopt a simple monopole expression for the charge form factor (with $\Lambda^2 = 6/R_C^2$) that reproduces the leading term in the small- \mathbf{k} -expansion. We assume the same form factor in \mathbf{C}_{tree} for simplicity:

$$\mathbf{C}_{\gamma g}(\mathbf{k}) \approx \frac{\Lambda^2}{\Lambda^2 + \mathbf{k}^2}, \quad \mathbf{C}_{\text{tree}}(\mathbf{k}) \approx \mathbf{C}_0^A \frac{\Lambda^2}{\Lambda^2 + \mathbf{k}^2}, \quad (14)$$

since no extra information of the latter is currently available. With these, the integrals I^0 , I' can be evaluated

analytically, and the squared amplitude $|\mathcal{M}_{\gamma W}|^2$ as well as the tree-loop interference $2|\mathcal{M}_{\text{tree}}^* \mathcal{M}_{\gamma W}|$, after averaging and summing over initial and final spins, are found to be:

$$\begin{aligned} |\overline{\mathcal{M}_{\gamma W}}|^2 &\approx \frac{4M_i M_f}{2J_i + 1} \frac{3\pi}{2} G_F^2 V_{ud}^2 (Z_f \alpha)^2 |\mathfrak{C}_0^A|^2 E_e E_\nu \\ &\times \left\{ 8E_e^2 L^2 - \frac{\mathbf{p}_e^2}{32} (4L - 3) (44L + 15) \right. \\ &\left. + \vec{\beta} \cdot \hat{\mathbf{p}}_\nu \left[6E_e^2 L + \frac{5\mathbf{p}_e^2}{32} (4L - 3)^2 \right] \right\} \\ 2\Re\{\overline{\mathcal{M}_{\text{tree}}^* \mathcal{M}_{\gamma W}}\} &\approx -\frac{4M_i M_f}{2J_i + 1} \frac{3\pi}{2} G_F^2 V_{ud}^2 Z_f \alpha |\mathfrak{C}_0^A|^2 \mathbf{q} \\ &\times \sin \theta_{e\mathbf{q}} \left\{ 16E_e^2 E_\nu L - 2E_e \mathbf{p}_e^2 (4L + 3) \right. \\ &\left. + E_e \mathbf{p}_e \cdot \mathbf{q} \cos \theta_{e\mathbf{q}} (20L + 9) - 2E_\nu \mathbf{p}_e^2 (4L - 3) \right\}, \quad (15) \end{aligned}$$

where $L \equiv \ln(\Lambda/\mathbf{p}_e)$ [79]. The appearance of the angle $\theta_{e\mathbf{q}} \equiv \cos^{-1}(\hat{\mathbf{p}}_e \cdot \hat{\mathbf{q}})$ in the second expression is because one needs to re-align the nuclear polarization direction in $\mathcal{M}_{\text{tree}}$ from $\hat{\mathbf{q}}$ to $\hat{\mathbf{p}}_e$ in order to interfere with $\mathcal{M}_{\gamma W}$ in Eq.(12). Recall that the result above is derived by taking $\vec{q} \approx \vec{0}$ in $T^{\mu\nu}$, and the non-vanishing of $|\overline{\mathcal{M}_{\gamma W}}|^2$ demonstrates our assertion at the beginning of this Letter. Notice, however, that one still keeps the finite \vec{q} in the momentum conservation $\vec{q} = \vec{p}_e + \vec{p}_\nu$, and Eq.(15) may still be applicable for small but non-zero values of \mathbf{q} .

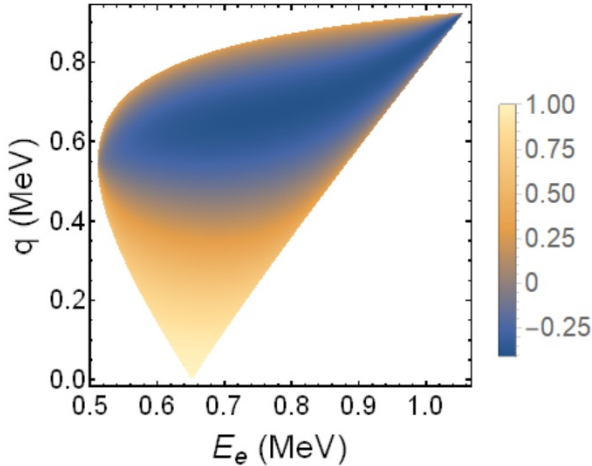


Figure 2: The Dalitz plot of $1 - |\overline{\mathcal{M}_{\text{tree}}}|^2 / |\overline{\mathcal{M}_{\text{tot}}}|^2$ for $^{90}\text{Sr} \rightarrow ^{90}\text{Y}$.

It is instructive to compare the radiative terms to the tree-level squared amplitude [16]:

$$\begin{aligned} |\overline{\mathcal{M}_{\text{tree}}}|^2 &\approx \frac{4M_i M_f}{2J_i + 1} 16\pi G_F^2 V_{ud}^2 |\mathfrak{C}_0^A|^2 E_e E_\nu \mathbf{q}^2 \\ &\times \left(\frac{5}{2} - \vec{\beta} \cdot \hat{\mathbf{p}}_\nu + \frac{\hat{\mathbf{p}}_\nu \cdot \hat{\mathbf{q}} \vec{\beta} \cdot \hat{\mathbf{q}}}{2} \right). \quad (16) \end{aligned}$$

We do this for the transition $^{90}\text{Sr} \rightarrow ^{90}\text{Y}$, which is interesting due to its large Z_f and a particularly small Q_β -value

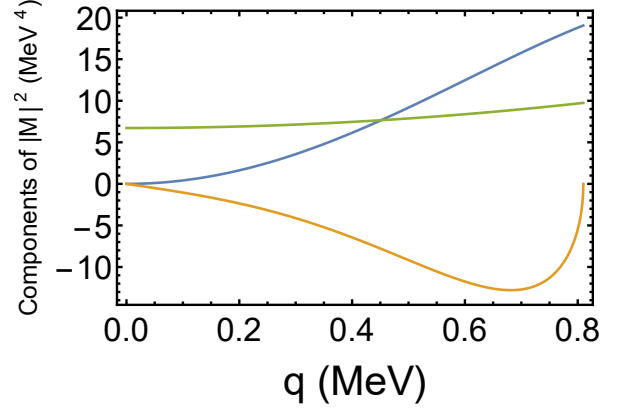


Figure 3: The plot of $|\overline{\mathcal{M}_{\text{tree}}}|^2$ (blue), $2\Re\{\overline{\mathcal{M}_{\text{tree}}^* \mathcal{M}_{\gamma W}}\}$ (orange) and $|\overline{\mathcal{M}_{\gamma W}}|^2$ (green) at fixed E_e for $^{90}\text{Sr} \rightarrow ^{90}\text{Y}$, scaling out the constant $4M_i M_f G_F^2 V_{ud}^2 |\mathfrak{C}_0^A|^2 / (2J_i + 1)$.

of 545.9(14) keV; $R_C \approx 4.26$ fm is taken for the nuclear radius [80]. First, we plot the quantity $1 - |\overline{\mathcal{M}_{\text{tree}}}|^2 / |\overline{\mathcal{M}_{\text{tot}}}|^2$ in the full 3-body phase space (\mathcal{D}_3) spanned by E_e and \mathbf{q} :

$$\begin{aligned} C(\mathbf{q}) - D(\mathbf{q}) < E_e < C(\mathbf{q}) + D(\mathbf{q}) \\ 0 < \mathbf{q} < \sqrt{E_{f,\text{max}}^2 - M_f^2} \quad (17) \end{aligned}$$

where

$$\begin{aligned} C(\mathbf{q}) &= \frac{(M_i - E_f)(M_i^2 + m_e^2 + M_f^2 - 2E_f M_i)}{2(M_i^2 + M_f^2 - 2E_f M_i)} \\ D(\mathbf{q}) &= \frac{\mathbf{q}(M_i^2 + M_f^2 - m_e^2 - 2E_f M_i)}{2(M_i^2 + M_f^2 - 2E_f M_i)} \\ E_{f,\text{max}} &= \frac{M_i^2 - m_e^2 + M_f^2}{2M_i}, \quad (18) \end{aligned}$$

with $E_f \equiv \sqrt{M_f^2 + \mathbf{q}^2}$, and $|\overline{\mathcal{M}_{\text{tot}}}|^2$ sums the three terms in Eqs.(15) and (16). From Fig.2 it is clearly seen that the size of the radiative corrections is substantial, and overtakes the tree-level contribution in the small- \mathbf{q} region which constitutes a significant portion of the entire phase space.

In Fig.3 we plot the various terms in Eqs.(15), (16) on a fixed-energy slice in the phase space: $E_e = ((M_i - M_f)^2 + m_e^2) / (2(M_i - M_f))$, that includes the $\mathbf{q} = 0$ point. One sees that, at $\mathbf{q} \rightarrow 0$ the tree-level squared amplitude and the interference term decay as \mathbf{q}^2 and \mathbf{q} respectively, while $|\overline{\mathcal{M}_{\gamma W}}|^2$ approaches a constant, which leads to its dominance at the small- \mathbf{q} region, in stark contrast to the traditional understanding of forbidden decays; therefore, any precision study of the decay shape without including the RC would be premature. We can also study the effect of RC on the total decay rate using the formula:

$$\Gamma = \frac{1}{64\pi^3 M_i} \int_{\mathcal{D}_3} dE_e d\mathbf{q} \frac{\mathbf{q}}{E_f} |\mathcal{M}|^2. \quad (19)$$

For $^{90}\text{Sr} \rightarrow ^{90}\text{Y}$, we obtain $1 - \Gamma_{\text{tree}}/\Gamma_{\text{tot}} \approx -7.7\%$, indicating a somewhat smaller correction to the total rate compared to the decay shape; this is due to a partial cancellation between the orange and green lines in Fig.3, which is purely accidental. One can also study the correction to the beta spectrum, as we present in the supplementary material. Notice that the \mathbf{q} -integrated results should be taken with a grain of salt as our approximate formula becomes inaccurate in the high- \mathbf{q} region. We defer the more comprehensive analysis at arbitrary \mathbf{q} to a later work.

In conclusion, we have shown that the existing understanding of decay kinematics in forbidden nuclear transitions has to be thoroughly revisited; the thought-to-be forbidden region of $\mathbf{q} \approx 0$ is opened up by RC, and depending on the specific transition the RC contribution may even be larger than the tree-level in a wider kinematic region. On the one hand, this imposes an extra challenge to the theory community due to the need to compute \mathbf{k} -dependent nuclear matrix elements, for instance $\mathcal{C}_{\text{tree}}(\mathbf{k})$, using reliable *ab initio* methods in order to correctly interpret forbidden beta decay data. On the other hand, our work also unveils a number of new experimental opportunities and discovery potential. By focusing on the small- \mathbf{q} region, one effectively evades the large tree-level uncertainty and has a direct experimental probe of the RC physics. It is also interesting to notice that, the topologies in Fig.1 that open up the forbidden decay at $\mathbf{q} = 0$ are not only achievable within the SM, but also with new physics. While modifications to the charged-current interactions induced by heavy new physics do not work [16], light new DOFs can play a similar role as the SM photon and open up the decay at $\mathbf{q} = 0$. Therefore, forbidden decays at small \mathbf{q} provide a perfect avenue to study such light new DOFs, provided that the SM RC in this region is computed to a moderate accuracy. We hope these findings provide new motivations for future theoretical and experimental programs in this topic.

We thank Oscar Naviliat-Cuncic, Mikhail Gorchtein, Leendert Hayen, Charlie Rasco and Guy Ron for inspiring discussions. C.-Y.S. and A.G.-M. are supported in part by the U.S. Department of Energy (DOE), Office of Science, Office of Nuclear Physics, under award DE-FG02-97ER41014. Additionally, C.-Y.S. receives support from the FRIB Theory Alliance award DE-SC0013617, and A.G.-M. is supported by the DOE Topical Collaboration "Nuclear Theory for New Physics", award No. DE-SC0023663, and the Hebrew University of Jerusalem through the Dalia and Dan Maydan Post-Doctoral Fellowship. V.C. is supported by the U.S. DOE Office of Science, Office of Nuclear Physics, under Grant No. DE-FG02-00ER41132.

-
- [1] M. Gorchtein and C. Y. Seng, Superallowed nuclear beta decays and precision tests of the Standard Model, *Ann. Rev. Nucl. Part. Sci.* **74**, 23 (2024), arXiv:2311.00044 [nucl-th].
 - [2] N. Cabibbo, Unitary Symmetry and Leptonic Decays, *Meeting of the Italian School of Physics and Weak Interactions Bologna, Italy, April 26-28, 1984*, *Phys. Rev. Lett.* **10**, 531 (1963).
 - [3] M. Kobayashi and T. Maskawa, CP Violation in the Renormalizable Theory of Weak Interaction, *Prog. Theor. Phys.* **49**, 652 (1973).
 - [4] V. Cirigliano, M. Gonzalez-Alonso, and M. L. Graesser, Non-standard Charged Current Interactions: beta decays versus the LHC, *JHEP* **02**, 046, arXiv:1210.4553 [hep-ph].
 - [5] V. Cirigliano, S. Gardner, and B. Holstein, Beta Decays and Non-Standard Interactions in the LHC Era, *Prog. Part. Nucl. Phys.* **71**, 93 (2013), arXiv:1303.6953 [hep-ph].
 - [6] M. Gonzalez-Alonso, O. Naviliat-Cuncic, and N. Severijns, New physics searches in nuclear and neutron β decay, *Prog. Part. Nucl. Phys.* **104**, 165 (2019), arXiv:1803.08732 [hep-ph].
 - [7] V. Cirigliano, W. Dekens, J. de Vries, E. Mereghetti, and T. Tong, Anomalies in global SMEFT analyses: a case study of first-row CKM unitarity, (2023), arXiv:2311.00021 [hep-ph].
 - [8] C. H. Johnson, F. Pleasonton, and T. A. Carlson, Precision measurement of the recoil energy spectrum from the decay of He^6 , *Phys. Rev.* **132**, 1149 (1963).
 - [9] F. Glück, Order- α radiative correction to 6He and 32Ar β decay recoil spectra, *Nucl. Phys. A* **628**, 493 (1998).
 - [10] A. Glick-Magid, C. Forssén, D. Gazda, D. Gazit, P. Gysbers, and P. Navrátil, Nuclear *ab initio* calculations of 6He β -decay for beyond the standard model studies, *Phys. Lett. B* **832**, 137259 (2022).
 - [11] P. Müller, Y. Bagdasarova, R. Hong, A. Leredde, K. Bailey, X. Fléchar, A. Garcia, B. Graner, A. Knecht, O. Naviliat-Cuncic, *et al.*, β -nuclear-recoil correlation from $\text{He} 6$ decay in a laser trap, *Phys. Rev. Lett.* **129**, 182502 (2022).
 - [12] Y. Mishnayot, A. Glick-Magid, H. Rahangdale, M. Hass, B. Ohayon, A. Gallant, N. D. Scielzo, S. Vaintraub, R. O. Hughes, T. Hirsch, C. Forssén, D. Gazda, P. Gysbers, J. Menéndez, P. Navrátil, L. Weissman, V. Srivastava, A. Kreisel, B. Kaizer, H. Dafna, M. Buzaglo, D. Gazit, J. T. Harke, and G. Ron, **Constraining new physics with a measurement of the ^{23}Ne β -decay branching ratio** 10.48550/arxiv.2107.14355 (*arXiv:2107.14355*).
 - [13] B. Longfellow, A. Gallant, G. Sargsyan, M. Burkey, T. Hirsh, G. Savard, N. Scielzo, L. Varriano, M. Brodeur, D. Burdette, *et al.*, Improved tensor current limit from b 8 β decay including new recoil-order calculations, *Phys. Rev. Lett.* **132**, 142502 (2024).
 - [14] M. Brodeur, N. Buzinsky, M. A. Caprio, V. Cirigliano, J. A. Clark, P. J. Fasano, J. A. Formaggio, A. T. Gallant, A. Garcia, S. Gandolfi, S. Gardner, A. Glick-Magid, L. Hayen, H. Hergert, J. D. Holt, M. Horoi, M. Y. Huang, K. D. Launey, K. G. Leach, B. Longfellow, A. Lovato, A. E. McCoy, D. Melconian, P. Mohanmurthy, D. C. Moore, P. Mueller, E. Mereghetti, W. Mittig, P. Navrátil, S. Pastore, M. Piarulli, D. Puentes, B. C. Rasco, M. Redshaw,

- G. H. Sargsyan, G. Savard, N. D. Scielzo, C. Y. Seng, A. Shindler, S. R. Stroberg, J. Surbrook, A. Walker-Loud, R. B. Wiringa, C. Wrede, A. R. Young, and V. Zelevinsky, Nuclear β decay as a probe for physics beyond the standard model 10.48550/arXiv.2301.03975 (2023), arXiv:2301.03975 [nucl-ex].
- [15] T. D. Lee and C.-N. Yang, Question of Parity Conservation in Weak Interactions, *Phys. Rev.* **104**, 254 (1956).
- [16] A. Glick-Magid, Y. Mishnayot, I. Mukul, M. Hass, S. Vaintraub, G. Ron, and D. Gazit, Beta spectrum of unique first-forbidden decays as a novel test for fundamental symmetries, *Phys. Lett. B* **767**, 285 (2017), arXiv:1609.03268 [nucl-ex].
- [17] A. Glick-Magid and D. Gazit, Multipole decomposition of tensor interactions of fermionic probes with composite particles and bsm signatures in nuclear reactions, *Phys. Rev. D* **107**, 075031 (2023).
- [18] J. D. Jackson, S. B. Treiman, and H. W. Wyld, Coulomb corrections in allowed beta transitions, *Nucl. Phys.* **4**, 206 (1957).
- [19] J. D. Jackson, S. B. Treiman, and H. W. Wyld, Possible tests of time reversal invariance in Beta decay, *Phys. Rev.* **106**, 517 (1957).
- [20] I. Mardor, O. Aviv, M. Avriganu, D. Berkovits, A. Dahan, T. Dickel, I. Eliyahu, M. Gai, I. Gavish-Segev, S. Halfon, M. Hass, T. Hirsh, B. Kaiser, D. Kijel, A. Kreisel, Y. Mishnayot, I. Mukul, B. Ohayon, M. Paul, A. Perry, H. Rahangdale, J. Rodnizki, G. Ron, R. Sasson-Zukran, A. Shor, I. Silverman, M. Tessler, S. Vaintraub, and L. Weissman, The Soreq applied research accelerator facility (SARAF): Overview, research programs and future plans, *Eur. Phys. J. A* **54**, 91 (2018).
- [21] B. Ohayon, J. Chocron, T. Hirsh, A. Glick-Magid, Y. Mishnayot, I. Mukul, H. Rahangdale, S. Vaintraub, O. Heber, D. Gazit, and G. Ron, Weak interaction studies at SARAF, *Hyperfine Interact.* **239**, 57 (2018).
- [22] G. Ron, private communication (2024).
- [23] B. C. Rasco, private communication (2024).
- [24] P. Shuai, B. C. Rasco, K. P. Rykaczewski, A. Fijałkowska, M. Karny, M. Wolińska Cichocka, R. K. Grzywacz, C. J. Gross, D. W. Stracener, E. F. Zganjar, J. C. Batchelder, J. C. Blackmon, N. T. Brewer, S. Go, M. Cooper, K. C. Goetz, J. W. Johnson, C. U. Jost, T. T. King, J. T. Matta, J. H. Hamilton, A. Laminack, K. Miernik, M. Madurga, D. Miller, C. D. Nesaraja, S. Padgett, S. V. Paulauskas, M. M. Rajabali, T. Ruland, M. Stepaniuk, E. H. Wang, and J. A. Winger, Determination of β -decay feeding patterns of ^{88}Rb and ^{88}Kr using the modular total absorption spectrometer at ornl hribf, *Phys. Rev. C* **105**, 054312 (2022).
- [25] H. A. Weidenmuller, First-Forbidden Beta Decay, *Rev. Mod. Phys.* **33**, 574 (1961).
- [26] J. Damgaard, R. Broglia, and C. Riedel, First-forbidden beta-decays in the lead region, *Nucl. Phys. A* **135**, 310 (1969).
- [27] G. Bertsch and A. Molinari, Correlation effect on unique forbidden decays, *Nucl. Phys. A* **148**, 87 (1970).
- [28] H. A. Smith and P. C. Simms, Nuclear matrix elements in the first forbidden beta decay of 198 Au, *Nucl. Phys. A* **159**, 143 (1970).
- [29] J. D. Vergados, First-forbidden unique β -decays in the Sr region, *Nucl. Phys. A* **166**, 285 (1971).
- [30] C. W. E. Van Eijk, Nuclear matrix elements for the first-forbidden β -decay of 198 Au, *Nucl. Phys. A* **169**, 239 (1971).
- [31] J. S. Schweitzer and P. C. Simms, A comparison of methods for determining nuclear matrix elements in first-forbidden β -decay, *Nucl. Phys. A* **198**, 481 (1972).
- [32] H. A. Smith, Nuclear Matrix Elements in the First-Forbidden Beta Decay of Hg-203, *Phys. Rev. C* **5**, 1732 (1972).
- [33] J. S. Schweitzer and P. C. Simms, Nuclear matrix elements in the first-forbidden β -decay of 125 Sb, *Nucl. Phys. A* **202**, 602 (1973).
- [34] H. A. Smith, J. S. Schweitzer, and P. C. Simms, Nuclear matrix elements in the first-forbidden β -decays of 122 Sb and 124 Sb, *Nucl. Phys. A* **211**, 473 (1973).
- [35] S. Lakshminarayana, M. S. Rao, L. Raghavendra Rao, V. S. Rao, and D. L. Sastry, Nuclear matrix elements governing the 693 keV first-forbidden beta transition in the decay of Ag-111, *Phys. Rev. C* **24**, 2260 (1981).
- [36] W. Becker, R. R. Schlicher, and M. O. Scully, Forbidden nuclear β -decay in an intense plane-wave field, *Nucl. Phys. A* **426**, 125 (1984).
- [37] O. Civitarese, F. Krmpotić, and O. A. Rosso, Collective effects induced by charge-exchange vibrational modes on $0^- \rightarrow 0^+$ and $2^- \rightarrow 0^+$ first-forbidden β -decay transitions, *Nucl. Phys. A* **453**, 45 (1986).
- [38] E. K. Warburton, Core polarization effects on spin-dipole and first-forbidden beta-decay operators in the lead region, *Phys. Rev. C* **42**, 2479 (1990).
- [39] E. K. Warburton, First-forbidden beta decay in the lead region and mesonic enhancement of the weak axial current, *Phys. Rev. C* **44**, 233 (1991).
- [40] E. K. Warburton, Second-forbidden unique beta decays of Be-10, Na-22, and Al-26, *Phys. Rev. C* **45**, 463 (1992).
- [41] J. Suhonen, Calculation of allowed and first-forbidden beta-decay transitions of odd-odd nuclei, *Nucl. Phys. A* **563**, 205 (1993).
- [42] G. Martinez-Pinedo and P. Vogel, Shell model calculation of the beta- and beta+ partial half-lives of 54mn and other unique second forbidden beta decays, *Phys. Rev. Lett.* **81**, 281 (1998), arXiv:nucl-th/9803032.
- [43] I. N. Borzov, Gamow-Teller and first forbidden decays near the r process paths at $N = 50$, $N = 82$, and $N = 126$, *Phys. Rev. C* **67**, 025802 (2003).
- [44] M. T. Mustonen, M. Aunola, and J. Suhonen, Theoretical description of the fourth-forbidden non-unique beta decays of Cd-113 and In-115, *Phys. Rev. C* **73**, 054301 (2006), [Erratum: *Phys.Rev.C* 76, 019901 (2007)].
- [45] M. Haaranen, M. Horoi, and J. Suhonen, Shell-model study of the 4th- and 6th-forbidden β -decay branches of Ca48, *Phys. Rev. C* **89**, 034315 (2014).
- [46] D.-L. Fang and B. A. Brown, Effect of first forbidden decays on the shape of neutrino spectra, *Phys. Rev. C* **91**, 025503 (2015), [Erratum: *Phys.Rev.C* 93, 049903 (2016)], arXiv:1502.02246 [nucl-th].
- [47] J.-U. Nabi, N. Çakmak, and Z. Iftikhar, First-forbidden β -decay rates, energy rates of β -delayed neutrons and probability of β -delayed neutron emissions for neutron-rich nickel isotopes, *Eur. Phys. J. A* **52**, 5 (2016), arXiv:1602.06381 [nucl-th].
- [48] M. Haaranen, P. C. Srivastava, and J. Suhonen, Forbidden nonunique β decays and effective values of weak coupling constants, *Phys. Rev. C* **93**, 034308 (2016).
- [49] J.-U. Nabi, N. Çakmak, M. Majid, and C. Selam, Unique first-forbidden β -decay transitions in odd-odd and even-even heavy nuclei, *Nucl. Phys. A* **957**, 1 (2017).

- [50] J. Kostensalo and J. Suhonen, g_A -driven shapes of electron spectra of forbidden β decays in the nuclear shell model, *Phys. Rev. C* **96**, 024317 (2017).
- [51] A. Kumar, P. C. Srivastava, J. Kostensalo, and J. Suhonen, Second-forbidden nonunique β^- decays of Na24 and Cl36 assessed by the nuclear shell model, *Phys. Rev. C* **101**, 064304 (2020), arXiv:2007.08122 [nucl-th].
- [52] A. Kumar and P. C. Srivastava, Shell-model description for the first-forbidden β^- decay of ^{207}Hg into the one-proton-hole nucleus ^{207}Tl , *Nucl. Phys. A* **1014**, 122255 (2021), arXiv:2105.07781 [nucl-th].
- [53] A. Glick-Magid and D. Gazit, A formalism to assess the accuracy of nuclear-structure weak interaction effects in precision β -decay studies, *J. Phys. G* **49**, 105105 (2022), arXiv:2107.10588 [nucl-th].
- [54] S. Sharma, P. C. Srivastava, A. Kumar, and T. Suzuki, Shell-model description for the properties of the forbidden β^- decay in the region “northeast” of $\text{Pb}208$, *Phys. Rev. C* **106**, 024333 (2022), arXiv:2207.06259 [nucl-th].
- [55] S. Sharma, P. C. Srivastava, and A. Kumar, Forbidden beta decay properties of $^{135,137}\text{Te}$ using shell-model, *Nucl. Phys. A* **1031**, 122596 (2023), arXiv:2212.13870 [nucl-th].
- [56] B.-L. Wang and L.-J. Wang, First-forbidden transition of nuclear β decay by projected shell model, *Phys. Lett. B* **850**, 138515 (2024), arXiv:2310.19523 [nucl-th].
- [57] A. Kumar, N. Shimizu, Y. Utsuno, C. Yuan, and P. C. Srivastava, Large-scale shell model study of β^- -decay properties of $N=126, 125$ nuclei: Role of Gamow-Teller and first-forbidden transitions in the half-lives, *Phys. Rev. C* **109**, 064319 (2024).
- [58] A. Saxena and P. C. Srivastava, Higher forbidden unique β^- decay transitions and shell-model interpretation, *Nucl. Phys. A* **1051**, 122939 (2024).
- [59] G. De Gregorio, R. Mancino, L. Coraggio, and N. Itaco, Forbidden β decays within the realistic shell model, *Phys. Rev. C* **110**, 014324 (2024), arXiv:2403.02272 [nucl-th].
- [60] A. Glick-Magid, C. Forssén, D. Gazda, D. Gazit, L. Jokiniemi, K. Kravvaris, and P. Navrátil, Ab initio calculations of unique first-forbidden beta-decay of ^{16}n for bsm searches, work in preparation (2024).
- [61] C.-Y. Seng, M. Gorchtein, H. H. Patel, and M. J. Ramsey-Musolf, Reduced Hadronic Uncertainty in the Determination of V_{ud} , *Phys. Rev. Lett.* **121**, 241804 (2018), arXiv:1807.10197 [hep-ph].
- [62] C. Y. Seng, M. Gorchtein, and M. J. Ramsey-Musolf, Dispersive evaluation of the inner radiative correction in neutron and nuclear β decay, *Phys. Rev. D* **100**, 013001 (2019), arXiv:1812.03352 [nucl-th].
- [63] K. Shiells, P. G. Blunden, and W. Melnitchouk, Electroweak axial structure functions and improved extraction of the V_{ud} CKM matrix element, *Phys. Rev. D* **104**, 033003 (2021), arXiv:2012.01580 [hep-ph].
- [64] C.-Y. Seng, Radiative Corrections to Semileptonic Beta Decays: Progress and Challenges, *Particles* **4**, 397 (2021), arXiv:2108.03279 [hep-ph].
- [65] M. Gorchtein and C.-Y. Seng, The Standard Model Theory of Neutron Beta Decay, *Universe* **9**, 422 (2023), arXiv:2307.01145 [hep-ph].
- [66] V. Cirigliano, W. Dekens, E. Mereghetti, and O. Tomalak, Effective field theory for radiative corrections to charged-current processes: Vector coupling, *Phys. Rev. D* **108**, 053003 (2023), arXiv:2306.03138 [hep-ph].
- [67] V. Cirigliano, W. Dekens, J. de Vries, S. Gandolfi, M. Hoferichter, and E. Mereghetti, Ab-initio electroweak corrections to superallowed β decays and their impact on V_{ud} , (2024), arXiv:2405.18464 [nucl-th].
- [68] V. Cirigliano, W. Dekens, J. de Vries, S. Gandolfi, M. Hoferichter, and E. Mereghetti, Radiative corrections to superallowed β decays in effective field theory, (2024), arXiv:2405.18469 [hep-ph].
- [69] M. Gennari, M. Drissi, M. Gorchtein, P. Navrátil, and C.-Y. Seng, An *ab initio* recipe for taming nuclear-structure dependence of V_{ud} : the $^{10}\text{C} \rightarrow ^{10}\text{B}$ superallowed transition, (2024), arXiv:2405.19281 [nucl-th].
- [70] L. Hayen, Standard model $\mathcal{O}(\alpha)$ renormalization of g_A and its impact on new physics searches, *Phys. Rev. D* **103**, 113001 (2021), arXiv:2010.07262 [hep-ph].
- [71] M. Gorchtein and C.-Y. Seng, Dispersion relation analysis of the radiative corrections to g_A in the neutron β -decay, *JHEP* **10**, 053, arXiv:2106.09185 [hep-ph].
- [72] V. Cirigliano, J. de Vries, L. Hayen, E. Mereghetti, and A. Walker-Loud, Pion-Induced Radiative Corrections to Neutron β Decay, *Phys. Rev. Lett.* **129**, 121801 (2022), arXiv:2202.10439 [nucl-th].
- [73] C.-Y. Seng, Hybrid analysis of radiative corrections to neutron decay with current algebra and effective field theory, *JHEP* **07**, 175, arXiv:2403.08976 [hep-ph].
- [74] R. J. Hill and R. Plestid, Field Theory of the Fermi Function, *Phys. Rev. Lett.* **133**, 021803 (2024), arXiv:2309.07343 [hep-ph].
- [75] R. J. Hill and R. Plestid, All orders factorization and the Coulomb problem, *Phys. Rev. D* **109**, 056006 (2024), arXiv:2309.15929 [hep-ph].
- [76] K. Borah, R. J. Hill, and R. Plestid, Renormalization of beta decay at three loops and beyond, *Phys. Rev. D* **109**, 113007 (2024), arXiv:2402.13307 [hep-ph].
- [77] J. D. Walecka, *Theoretical nuclear and subnuclear physics* (World Scientific, 2004).
- [78] Without an explicit calculation, one cannot exclude that the sum over the excited intermediate state may make up for the Z_f factor. However, even if this were the case, it is unlikely that such neglected terms exactly cancel the contribution we focus on here, absent a symmetry to enforce the cancellation. Moreover, in radiative corrections to other systems [69], no strong sensitivity to highly excited nuclear states is observed.
- [79] Using dimensional regularization one obtains the same result with the replacement $\ln \Lambda \rightarrow \ln \mu + \text{constant}$.
- [80] I. Angeli and K. P. Marinova, Table of experimental nuclear ground state charge radii: An update, *Atom. Data Nucl. Data Tabl.* **99**, 69 (2013).

SUPPLEMENTARY MATERIAL

Rotation of $J = 2$ spin states

The multipole expansion formalism of the Fourier-transformed current operators $J^\mu(\pm\vec{k})$ is built in the coordinate system with $\hat{z} \equiv \hat{k}$. This frame is problematic when applying to the external (spinful) nuclear state, because \vec{k} is an unobserved photon momentum to be integrated over which cannot be used to represent the direction of the observable external nuclear spin; an observable direction has to be chosen for the latter, and a

natural option is the direction of the electron momentum \hat{p}_e . At the same time, it is necessary to express both the current operators and the nuclear states in the same coordinate system (with $\hat{z} = \hat{k}$) in order to apply the Wigner-Eckart theorem. Therefore, a transformation matrix of the external nuclear spin state along \hat{p}_e and \hat{k} is needed. In this work we focus on $J = 2$ nuclear states:

$$|2, m(\hat{p}_e)\rangle = \sum_{m'=-2}^2 S_{m'm}(\theta) |2, m'(\hat{k})\rangle, \quad (\text{S1})$$

where m and m' are the magnetic quantum numbers along \hat{p}_e and \hat{k} , respectively. The matrix $S(\theta)$ reads:

$$S(\theta) = \begin{pmatrix} \cos^4 \frac{\theta}{2} & \cos^2 \frac{\theta}{2} \sin \theta & \sqrt{\frac{3}{8}} \sin^2 \theta & \sin^2 \frac{\theta}{2} \sin \theta & \sin^4 \frac{\theta}{2} \\ -\cos^2 \frac{\theta}{2} \sin \theta & \cos^2 \frac{\theta}{2} (2 \cos \theta - 1) & \sqrt{\frac{3}{2}} \cos \theta \sin \theta & \frac{1}{2} (\cos \theta - \cos 2\theta) & \sin^2 \frac{\theta}{2} \sin \theta \\ \sqrt{\frac{3}{8}} \sin^2 \theta & -\sqrt{\frac{3}{2}} \cos \theta \sin \theta & 1 - \frac{3}{2} \sin^2 \theta & \sqrt{\frac{3}{2}} \cos \theta \sin \theta & \sqrt{\frac{3}{8}} \sin^2 \theta \\ -\sin^2 \frac{\theta}{2} \sin \theta & \frac{1}{2} (\cos \theta - \cos 2\theta) & -\sqrt{\frac{3}{2}} \cos \theta \sin \theta & \cos^2 \frac{\theta}{2} (2 \cos \theta - 1) & \cos^2 \frac{\theta}{2} \sin \theta \\ \sin^4 \frac{\theta}{2} & -\sin^2 \frac{\theta}{2} \sin \theta & \sqrt{\frac{3}{8}} \sin^2 \theta & -\cos^2 \frac{\theta}{2} \sin \theta & \cos^4 \frac{\theta}{2} \end{pmatrix}, \quad (\text{S2})$$

RME	$i(2^-) \rightarrow f(0^+)$	$i(0^+) \rightarrow f(2^-)$
$\mathfrak{C}_{\text{tree}}$	$\frac{1}{\mathbf{k}} \langle f(0^+) L_2^A(\mathbf{k}) i(2^-) \rangle$	$\frac{1}{\mathbf{k}} \langle f(2^-) L_2^A(\mathbf{k}) i(0^+) \rangle$
$\mathfrak{C}_{\gamma g}^{i,f}$	$\frac{1}{Z_{i,f}} \langle J_{i,f} m_{i,f} J^0(\mathbf{k}) J_{i,f} m_{i,f} \rangle$	
$\mathfrak{C}_{\gamma 1}^X$	$\frac{1}{\mathbf{k}} \langle f(0^+) C_1^{\text{em}}(\mathbf{k}) f(1_X^-) \rangle$	$\frac{1}{\mathbf{k}} \langle f(2^-) C_1^{\text{em}}(\mathbf{k}) f(1_X^+) \rangle$
$\mathfrak{C}_{\gamma 2}^X$	$\frac{1}{\mathbf{k}} \langle i(1_X^+) C_1^{\text{em}}(\mathbf{k}) i(2^-) \rangle$	$\frac{1}{\mathbf{k}} \langle i(1_X^-) C_1^{\text{em}}(\mathbf{k}) i(0^+) \rangle$
\mathfrak{C}_{A1}^X	$\langle f(1_X^-) L_1^A(\mathbf{k}) i(2^-) \rangle$	$\langle f(1_X^+) L_1^A(\mathbf{k}) i(0^+) \rangle$
\mathfrak{C}_{A2}^X	$\langle f(0^+) L_1^A(\mathbf{k}) i(1_X^+) \rangle$	$\langle f(2^-) L_1^A(\mathbf{k}) i(1_X^-) \rangle$

Table SI: Definitions of modified reduced matrix elements.

where $\theta \equiv \cos^{-1}(\hat{p}_e \cdot \hat{k})$.

Reduced matrix elements

The reduced matrix element of a generic multipole operator $O_{Jm}(\mathbf{k})$ is defined through the Wigner-Eckart

theorem:

$$\langle J_f m_f | O_{Jm}(\mathbf{k}) | J_i m_i \rangle = (-1)^{J_f - m_f} \begin{pmatrix} J_f & J & J_i \\ -m_f & m & m_i \end{pmatrix} \times \langle J_f || O_J(\mathbf{k}) || J_i \rangle. \quad (\text{S3})$$

In our analysis we need multiple operators from the electromagnetic and the axial weak current, which we denote as O_{Jm}^{em} and O_{Jm}^A , respectively. It is also beneficial to scale out the leading \mathbf{k} - (and Z)-dependence and define a new set of reduced matrix elements that are non-zero at $\mathbf{k} = 0$; this is done in Table SI. In particular, we have $\mathfrak{C}_{\gamma W}^{i,f}(0) = 1$.

Full leading expression of $T^{\mu\nu}$

Here we display the full expression of $T^{\mu\nu}$ at leading order of the multipole expansion.

$$\begin{aligned}
T^{0i}(m) &= i\sqrt{4M_i M_f} \mathbf{k} \left[\sqrt{4\pi} \mathbf{e}_{\text{tree}} \left(\frac{Z_f \mathbf{e}_{\gamma g}^f}{k_0 + i\varepsilon} - \frac{Z_i \mathbf{e}_{\gamma g}^i}{k_0 - i\varepsilon} \right) + \sqrt{\frac{32}{5}} \pi \sum_X \left(\frac{\mathbf{e}_{\gamma 1}^X \mathbf{e}_{A1}^X}{M_f(1_X^\mp) - M_f - k_0 - i\varepsilon} \right. \right. \\
&\quad \left. \left. + \frac{\mathbf{e}_{\gamma 2}^X \mathbf{e}_{A2}^X}{M_i(1_X^\pm) - M_i + k_0 - i\varepsilon} \right) \right] \left\{ S_{0m}(\theta)(\bar{\epsilon}_0^*)^i \mp \frac{\sqrt{3}}{2} (S_{\mp 1m}(\theta)(\bar{\epsilon}_1^*)^i + S_{\pm 1m}(\theta)(\bar{\epsilon}_{-1}^*)^i) \right\} \\
T^{ji}(m) &= i\pi \sqrt{\frac{32}{5}} \sqrt{4M_i M_f} \sum_X \left(\frac{(M_f(1_X^\mp) - M_f) \mathbf{e}_{\gamma 1}^X \mathbf{e}_{A1}^X}{M_f(1_X^\mp) - M_f - k_0 - i\varepsilon} + \frac{(M_i - M_i(1_X^\pm)) \mathbf{e}_{\gamma 2}^X \mathbf{e}_{A2}^X}{M_i(1_X^\pm) - M_i + k_0 - i\varepsilon} \right) \times \\
&\quad \left\{ (\bar{\epsilon}_0^*)^j \left[S_{0m}(\theta)(\bar{\epsilon}_0^*)^i \mp \frac{\sqrt{3}}{2} S_{\mp 1m}(\theta)(\bar{\epsilon}_1^*)^i \mp \frac{\sqrt{3}}{2} S_{\pm 1m}(\theta)(\bar{\epsilon}_{-1}^*)^i \right] \right. \\
&\quad + (\bar{\epsilon}_1^*)^j \left[\mp \frac{\sqrt{3}}{2} S_{\mp 1m}(\theta)(\bar{\epsilon}_0^*)^i + \sqrt{\frac{3}{2}} S_{\mp 2m}(\theta)(\bar{\epsilon}_1^*)^i + \frac{1}{2} S_{0m}(\theta)(\bar{\epsilon}_{-1}^*)^i \right] \\
&\quad \left. + (\bar{\epsilon}_{-1}^*)^j \left[\mp \frac{\sqrt{3}}{2} S_{\pm 1m}(\theta)(\bar{\epsilon}_0^*)^i + \frac{1}{2} S_{0m}(\theta)(\bar{\epsilon}_1^*)^i + \sqrt{\frac{3}{2}} S_{\pm 2m}(\theta)(\bar{\epsilon}_{-1}^*)^i \right] \right\} \tag{S4}
\end{aligned}$$

Correction to the beta spectrum

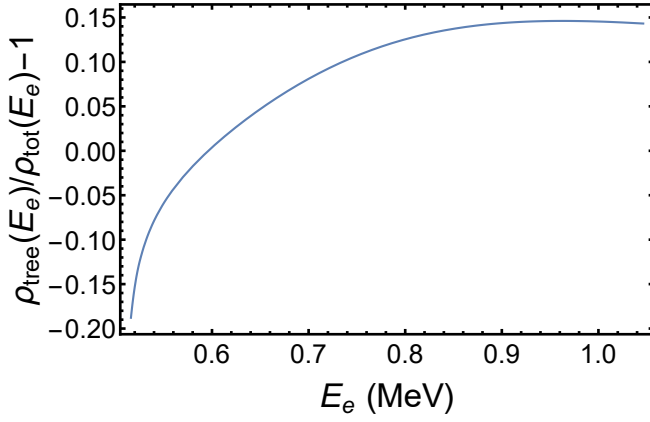


Figure S1: The correction to the beta spectrum for $^{90}\text{Sr} \rightarrow ^{90}\text{Y}$.

By performing the \mathbf{q} -integral in Eq.(19) and leaving E_e unintegrated, we can also study the RC to the beta spectrum, which we plot in Fig.S1 for $^{90}\text{Sr} \rightarrow ^{90}\text{Y}$.